Journal of Alloys and Compounds 520 (2012) 238–243

Contents lists available at SciVerse ScienceDirect

Journal of Alloys and Compounds

journal homepage: www.elsevier.com/locate/jallcom

Structural investigation on silver phosphate glasses embedded with nanoparticles

S. Kabi, A. Ghosh*

Department of Solid State Physics, Indian Association for the Cultivation of Science, Jadavpur, Kolkata 700032, India

ARTICLE INFO

Article history:
Received 24 November 2011
Received in revised form
28 December 2011
Accepted 4 January 2012
Available online 13 January 2012

Keywords:
Glass-nanocomposites
Microstructure
Optical properties
Thermal properties

ABSTRACT

Structural investigations of CdI_2 doped silver phosphate glass-nanocomposites in the system $xCdI_2$–$(1-x)(yAg_2O$–$(1-y)P_2O_5)$ are presented in this paper. Although, X-ray diffraction patterns show amorphous nature of the compositions, electron microscopic studies show several nanocrystalline phases such as CdI_2, β-AgI, $AgPO_3$ and $Ag_4P_2O_7$ dispersed within the glass matrix. The presence of CdI_2 nanoparticles in cluster form is dominant for the compositions in the limit of the glass forming domain. The particle size in polyphosphate compositions is higher than that of metaphosphate or ultraphosphate compositions. FTIR spectra of these compositions have been investigated. It has been observed that the presence of different nanocrystalline phases does not affect the basic glass network. Differential scanning calorimetric results show that the incorporation of CdI_2 within the glassy matrix increases the glass transition temperature. It is observed that the structural characteristics of the CdI_2 doped silver phosphate glasses are quite different from that of other divalent metal iodide doped glasses.

1. Introduction

Ion conducting glasses are highly interesting because of their potential application in solid state electrochemical devices such as batteries, sensors and smart windows [1]. Incorporation of AgI in silver phosphate glasses leads to high ionic conductivity [2]. Similarly, higher conductivity can also be achieved by introducing some divalent metal iodides (e.g. PbI_2, HgI_2, etc.) other than silver iodide in the glass network [1,2]. To look into this interesting phenomenon, it is necessary to have an insight on the microscopic structure of these glasses. It has been reported [2] that there is a coordination exchange between Ag^+ and Pb^{2+} ions in PbI_2 doped silver phosphate glasses, resulting in the formation of AgI cluster. The dissociation of Ag_2O depends on the type and amount of the dopant iodide salt [3]. In HgI_2 doped glasses the dissociation of Ag_2O is observed for HgI_2 content <20%, but beyond this limit HgI_2 remains unreacted within the glassy matrix [2]. However, in AgI or PbI_2 doped glasses the existence of AgI or PbI_2 clusters of significant size (10 Å) has been recently debated [1]. It has been observed that the incorporation of PbI_2 in the phosphate network leads to the coordination of Pb^{2+} ions with the non-bridging oxygen of the phosphate network. Simultaneously the Ag^+ ions from the phosphate chains are dissociated and are located in more salt like (i.e. Ag–I) environment [1].

Binary phosphate glasses xR_2O–$(1-x)P_2O_5$ (where R is alkali or silver) may be classified depending on the value of x. For $0 \le x \le 0.5$ the compositions are called ultraphosphate, for $x = 0.5$ the compositions are metaphosphate and for $x \ge 0.5$ the compositions are polyphosphate [4]. There are some reports on structural or electrical properties of divalent metal iodide (e.g. PbI_2, HgI_2, etc.) doped silver metaphosphate glasses [1,2,5]. In this paper, we have studied the structure of ultra, meta and polyphosphate glasses doped with different concentration of CdI_2. We have observed that the microstructure of these glasses is different from what was observed in the case of PbI_2 or HgI_2 doped phosphate glasses.

2. Experimental details

Samples of the compositions $xCdI_2$–$(1-x)(yAg_2O$–$(1-y)P_2O_5)$ [x = 0–0.20 for y = 0.60 series, x = 0–0.25 for y = 0.50 series and x = 0–0.40 for y = 0.40 series] were prepared by melt quenching technique. The reagent grade chemicals CdI_2, $AgNO_3$ and $NH_4H_2PO_4$ were mixed in appropriate molar ratio. They were ground thoroughly and mixed in a mortar. The mixtures were melted in alumina crucibles at 800–900 °C depending upon the composition. The melts were equilibrated for 2 h and then rapidly quenched between two aluminum blocks kept at room temperature. The samples of thickness in the range 0.5–0.8 mm were obtained. The undoped silver phosphate glasses are colorless and transparent, whereas CdI_2 doped samples are yellowish in color. The X-ray diffraction patterns of the powdered samples were recorded in an X-ray diffractometer (Bruker AXS, model D8 Advance) using Cu-K_α radiation (1.54 Å wavelength) at a scan rate of 0.02°/s. For transmission electron microscopic (TEM) studies the powdered samples were sonicated in acetone for 15 min in an ultrasonic bath (model EYELA) and the sonicated solution was dropped in a 300 mesh copper grid. The TEM images were taken in a high resolution transmission electron microscope (HR-TEM) (JEOL, model JEM 2010). The FTIR spectra in KBr matrices (sample:KBr = 1:100) were recorded in a spectrometer (model SHIMADZU 8400S) at room temperature. Calorimetric measurements were performed

* Corresponding author. Tel.: +91 3324734971; fax: +91 3324732805.
E-mail address: sspag@iacs.res.in (A. Ghosh).

0925-8388/$ – see front matter © 2012 Elsevier B.V. All rights reserved.
doi:10.1016/j.jallcom.2012.01.031

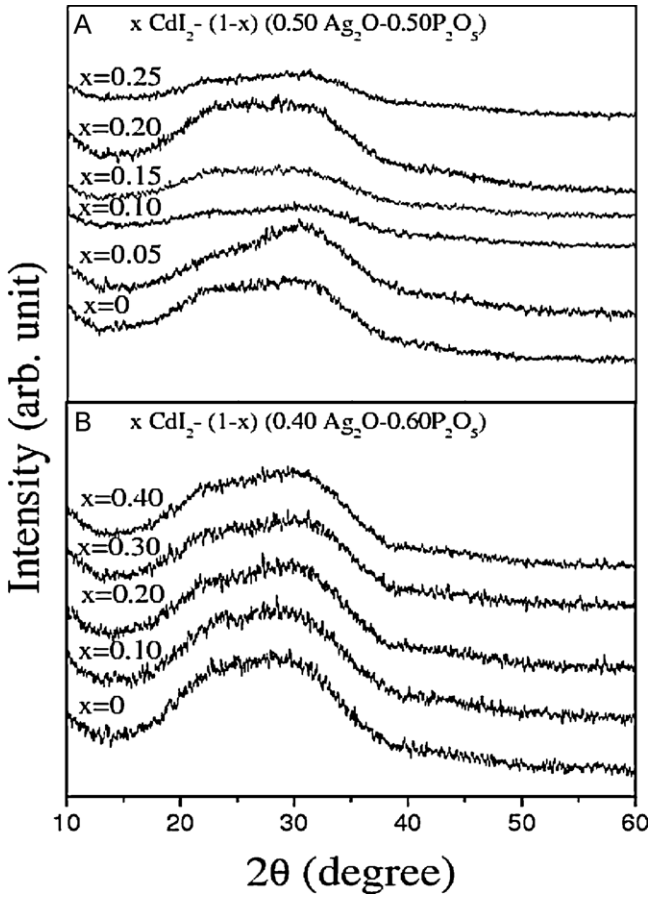

Fig. 1. Parts (a) and (b) show X-ray diffraction patterns of $x\mathrm{CdI_2}$–$(1-x)(y\mathrm{Ag_2O}$–$(1-y)\mathrm{P_2O_5})$ for the series $y = 0.50$ and 0.40, respectively.

in a differential scanning calorimeter (model PerkinElmer-DSC N-536-0022) under constant nitrogen flow (100 ml/min) with a scan rate of 10 °C/min.

3. Results and discussion

Fig. 1(a and b) represents the X-ray diffraction patterns of the compositions $x\mathrm{CdI_2}$–$(1-x)(y\mathrm{Ag_2O}$–$(1-y)\mathrm{P_2O_5})$ for the series $y = 0.50$ and 0.40, respectively. It is observed that all the samples exhibit amorphous nature. However, the electron microscopic studies (presented later) showed that several crystalline phases of size 5–50 nm depending upon the compositions are dispersed in the glassy matrix. The absence of diffraction peak for such X-ray amorphous compositions is generally due to small size and density of crystallites [6]. All prepared samples are glass-nanocomposites [6].

Typical TEM micrographs are shown in Fig. 2(a–d) for some compositions along with the selected area electron diffraction patterns shown in the inset. The micrographs show crystalline phases dispersed in the glassy matrix. It has been noted that $\mathrm{CdI_2}$ doped silver borophosphate glasses are also X-ray amorphous in nature, although several crystalline phases are embedded in the glass matrix [7].

The inter-planner spacing (d) was calculated from the selected area electron diffraction (SAED) patterns or crystalline fringe patterns, and comparing them with those given in the JCPDS-ICDD [8] data sheet the crystalline phases were determined. The calculated d-values and the corresponding crystalline phases for different series of the compositions are listed in Table 1.

It is observed that several crystalline phases such as $\mathrm{CdI_2}$, β-AgI, $\mathrm{Ag_4P_2O_7}$ and $\mathrm{AgPO_3}$ are embedded in the glass matrix depending upon the compositions. However, no crystalline phases were observed in the $x = 0$ composition of each series. It may be noted that $\mathrm{CdI_2}$ and β-AgI phases are present in all the compositions. The presence of $\mathrm{Ag_4P_2O_7}$ has been detected in $y = 0.60$ series while $\mathrm{AgPO_3}$ crystallites has been observed in $y = 0.40$ and 0.50 series. It is noteworthy [2] that the formation of AgI crystalline phase in $\mathrm{PbI_2}$–$\mathrm{AgPO_3}$ glasses is due to the exchange reaction between $\mathrm{Ag_2O}$ and $\mathrm{PbI_2}$. We expect that formation of β-AgI phases in our glasses is also due to the exchange reaction between $\mathrm{Ag_2O}$ and $\mathrm{CdI_2}$. It was proposed [2] that in $\mathrm{PbI_2}$–$\mathrm{AgPO_3}$ glasses $\mathrm{Pb^{2+}}$ ions are preferentially linked to the $\mathrm{PO_3}$ anions of the phosphate network, while $\mathrm{Ag^+}$ ions are linked with $\mathrm{I^-}$ ions producing AgI. The $\mathrm{CdI_2}$ crystalline phases imply the presence of some un-reacted $\mathrm{CdI_2}$. It should be noted that the presence of $\mathrm{CdI_2}$ is dominant [Fig. 2(c and d)] with respect to other crystalline phases for the compositions with highest $\mathrm{CdI_2}$ content. The selected area electron diffraction pattern shown in the inset of Fig. 2(c) reflects single crystalline nature of $\mathrm{CdI_2}$ particles [9]. High resolution TEM image and typical fast Fourier transform (FFT) pattern exhibited by $\mathrm{CdI_2}$ are also shown in the inset Fig. 2(d). The FFT pattern of $\mathrm{CdI_2}$ is similar to that reported earlier and it exhibits hexagonal nature of $\mathrm{CdI_2}$ crystallites [10].

The crystallites corresponding to β-AgI, $\mathrm{Ag_4P_2O_7}$ and $\mathrm{AgPO_3}$ phases are 30–50 nm in size [Fig. 2(a and b)]. On the other hand, the size of $\mathrm{CdI_2}$ crystallites is quite small (5–30 nm) [Fig. 2(c and d)]. The mean diameter of the $\mathrm{CdI_2}$ particles with particle count has been estimated from the particle size distribution for all the compositions. The histogram of the distribution of particle sizes is shown in Fig. 3 for a composition. The data were fitted to the lognormal distribution function given by [11].

$$f(r) = \frac{1}{\sqrt{2\pi}\ln\sigma}\exp\left\{-\frac{(\ln r - \ln\rho)}{2(\ln\sigma)^2}\right\} \quad (1)$$

where r is particle diameter, ρ is the geometric mean diameter and σ is the dimensionless geometric standard deviation. The average size of the particles obtained from fits is 17 nm (±2 nm) for $y = 0.60$ series. For $y = 0.50$ and 0.40 series the average size of the particles was obtained as 13 nm (±2 nm) and 11 nm (±2 nm), respectively. Thus, it is observed that the average size of the $\mathrm{CdI_2}$ particles for the compositions depends on the type of phosphate network. The average size of the particles in polyphosphate composition is higher than that of the metaphosphate and ultraphosphate compositions. The phosphate chain length in the polyphosphate compositions is smaller [4] and the glass network is quite weaker than those for the ultraphosphate compositions as observed from DSC studies presented later. Probably, this weak network structure assists in the nucleation and growth of $\mathrm{CdI_2}$ crystallites.

Fig. 4(a–c) shows FTIR spectra of the compositions $x\mathrm{CdI_2}$–$(1-x)(y\mathrm{Ag_2O}$–$(1-y)\mathrm{P_2O_5})$ for the series $y = 0.60$, 0.50 and 0.40, respectively. The band observed near 1243–1268 $\mathrm{cm^{-1}}$ for all the glass compositions is attributed to the asymmetric stretching vibration of $(\mathrm{PO_2})^-$ terminal of —O—$(\mathrm{PO_2})$— fragments[12]. This fragment is the monomer of the polymeric metaphosphate chain [12]. It should be mentioned that the absorption band of $(\mathrm{PO_2})^-$ group and P═O group generally overlap with each other [13]. The stretching frequency of P═O group is higher (1250 $\mathrm{cm^{-1}}$) in phosphorous rich ultraphosphate compositions ($y = 0.40$ series) compared to that (1233 $\mathrm{cm^{-1}}$) of the polyphosphate compositions ($y = 0.60$ series). This is probably due to strong localization of P═O in the central position of the interlinked phosphate tetrahedra for ultraphosphate glasses [14]. It is observed that as the amount of $\mathrm{CdI_2}$ content is increased, the overlapping of bands of $(\mathrm{PO_2})^-$ and P═O group becomes broader. This is due to the shifting of $(\mathrm{PO_2})^-$ stretching frequency to lower values [15].

The absorption band in the region 1080–1095 $\mathrm{cm^{-1}}$ appears for ultraphosphate and metaphosphate compositions ($y = 0.40$ and

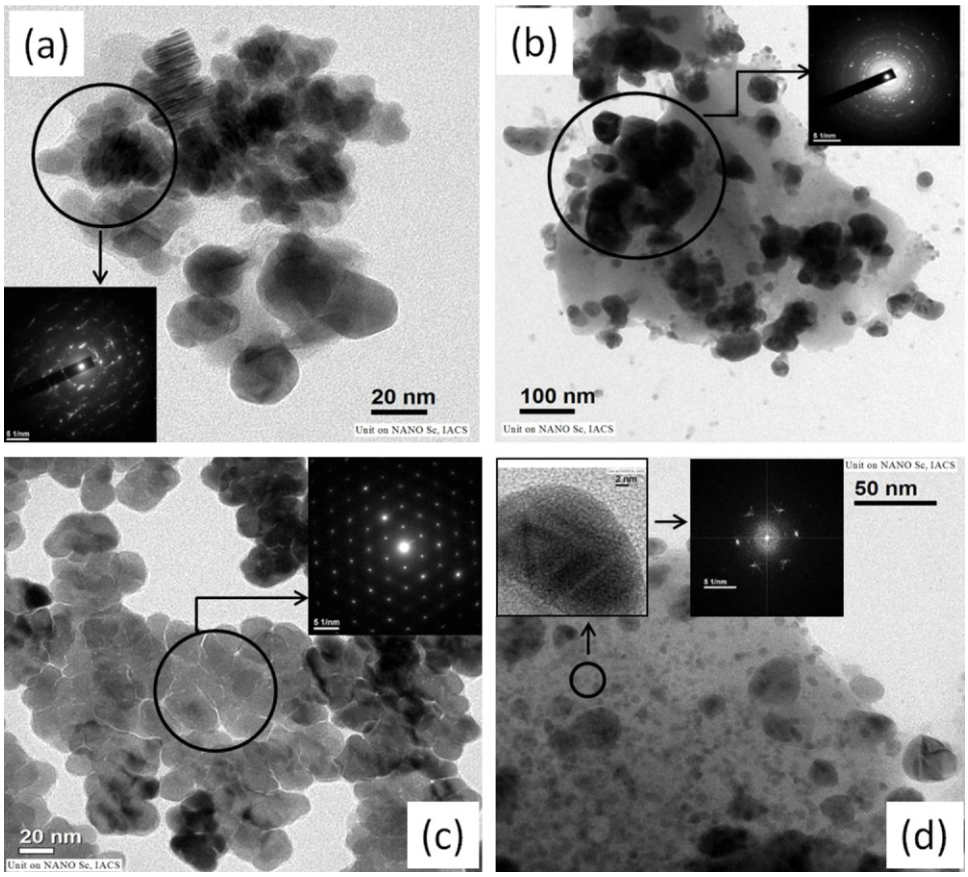

Fig. 2. Parts (a) and (b) show TEM micrograph for compositions ($x = 0.10$, $y = 0.60$) and ($x = 0.20$, $y = 0.40$), respectively. SAED patterns for selected zones are shown at the inset. (c) And (d) show distribution of CdI_2 particles for ($x = 0.20$, $y = 0.60$) and ($x = 0.40$, $y = 0.40$). SAED pattern for a selected zone is shown at the inset of (c). High resolution TEM image for a CdI_2 particle along with its FFT pattern is shown at the inset of (d).

Table 1
Inter-planer spacing (d) for different crystalline phase of $xCdI_2-(1-x)(yAg_2O-(1-y)P_2O_5)$ as obtained from TEM and their corresponding values along with reflecting planes given in the JCPDS data-sheet.

Compositions	Crystallites	d-value from TEM (Å)	d-value from JCPDS (Å)	Reflecting plane
$y = 0.60$	CdI_2	2.13	2.12	(1 1 0)
$x = 0.05–0.20$)		3.17	3.24	(1 0 1)
		2.04	2.03	(1 1 1)
		2.56	2.51	(1 0 2)
	β-AgI	2.30	2.30	(4 4 0)
		1.93	1.94	(6 3 0)
		1.59	1.61	(8 0 1)
	$Ag_4P_2O_7$	2.76	2.76	$(1\ 1\ \overline{1}\ 2)$
		1.59	1.60	$(1\ 1\ \overline{2}\ 4)$
		3.12	3.11	(1 1 1 0)
$y = 0.50$	CdI_2	3.24	3.24	(1 0 6)
$x = 0.05–0.25$)		2.82	2.86	(1 0 9)
		2.02	2.02	(1 1 6)
	β-AgI	1.97	1.94	(6 3 0)
		2.33	2.30	(4 4 0)
		3.69	3.68	(2 2 2)
	$AgPO_3$	3.98	4.06	
		3.52	3.51	
		3.47	3.45	
$y = 0.40$	CdI_2	2.83	2.86	(1 0 9)
$x = 0.10–0.40$)		2.04	2.02	(1 1 6)
		2.99	2.99	(1 0 8)
	$AgPO_3$	2.94	2.93	
		2.36	2.36	
		2.42	2.42	
	β-AgI	2.33	2.30	(4 4 0)
		3.74	3.68	(2 2 2)

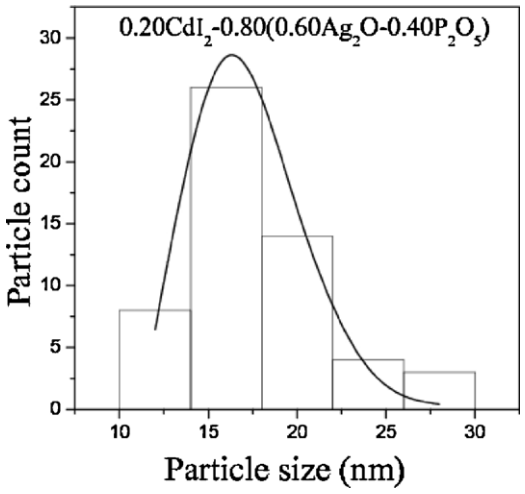

Fig. 3. Histogram for the particle distribution for the highest CdI_2 rich compositions for $y = 0.60$ series. The fit to the lognormal distribution is shown by the solid curve.

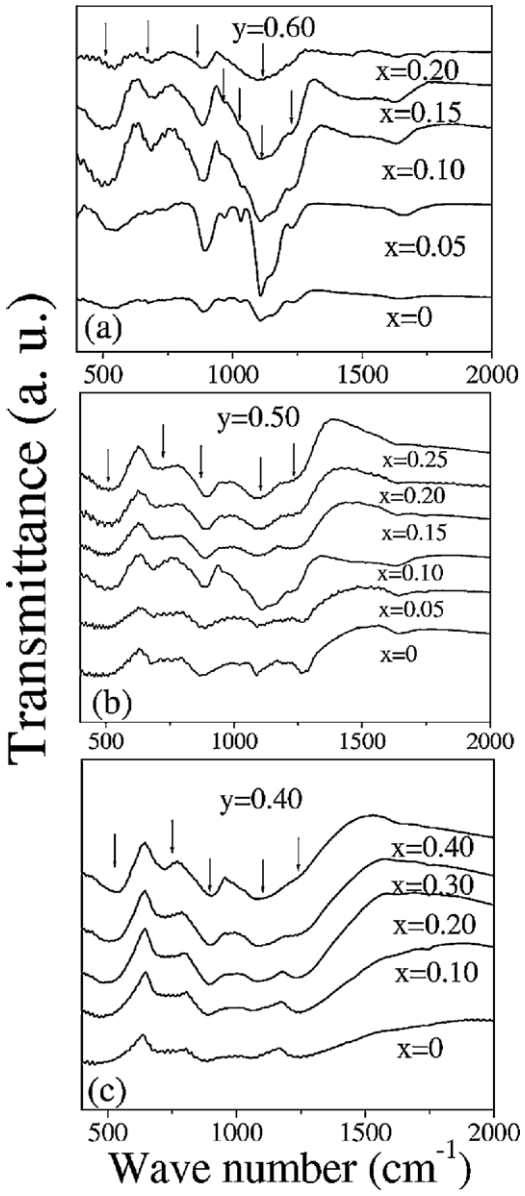

Fig. 4. Parts (a)–(c) show FTIR spectra for different compositions of $xCdI_2–(1-x)(yAg_2O–(1-y)P_2O_5)$ glass nanocomposites.

0.50 series). However, it is absent in polyphosphate ($y = 0.60$ series) glasses. This band has been assigned to the two different types of vibrational mode: one is due to the stretching of P—O^- group (chain terminator) and the other is the symmetric stretching of (PO_2) group [12]. In pure P_2O_5 glass this band appears at 1100 cm^{-1}, but due to the formation of P—O—Ag unit in silver phosphate glasses it appears at low frequency [14]. In the highest P_2O_5 rich glasses ($y = 0.40$ series), it is observed that, the absorption band (1080–1095 cm^{-1}) becomes more intense with increase of CdI_2 content. Generally, the relative intensity of bands changes due to the change in the percentage of different types of PO_4 tetrahedra present in the composition [13]. Insertions of CdI_2 into the glass network probably converts the PO_4 tetrahedra with three bridging oxygen to the PO_4 tetrahedra with two bridging oxygen i.e. three-dimensional network structure breaks into short metaphosphate chains [16]. In the metaphosphate compositions ($y = 0.50$), the absorption band (1080–1095 cm^{-1}) becomes broader as CdI_2 content is increased. This may be related to the shifting of (PO_2) stretching frequency to lower values [15] or due to formation of P—O—Cd covalent bond that increases the cross link density or in other way the rigidity of the glass network [17].

The asymmetric vibration of P—O—P bridge appears at 879–900 cm^{-1} and symmetric vibration of P—O—P bridge appears at 678–700 cm^{-1} for all the compositions [12]. It is observed that the stretching frequency shifts to the higher wave number with the increase of CdI_2 content. It was reported earlier that the covalent character of P—O—P bands increases and the bands become strengthened as more cadmium salts are added in the glass network [18].

For polyphosphate composition ($y = 0.60$) two bands appear at 1104 and 1169 cm^{-1}, respectively. These bands are due to low and high frequency component of asymmetric stretching of $(PO_3)^{2-}$ terminal group [12]. The intensity of the 1104 cm^{-1} band is higher than that of the 1169 cm^{-1} band. With the increase of CdI_2 concentration, the intensity of the 1169 cm^{-1} band decreases. However, the intensity of 1104 cm^{-1} band increases up to 20% CdI_2 content and then decreases. The variation of these bands is due to the redistribution of intensity between the low and high frequency component of $(PO_3)^{2-}$ terminal group [12]. The band at 1030 cm^{-1} (for $y = 0.60$ series) can be related to the symmetric stretching of $(PO_3)^{2-}$ terminal group. This band has almost disappeared for CdI_2 content $\geq$15%. There is a weak band at 969 cm^{-1} (for $y = 0.60$ series) which might be related to the symmetric stretch of the $(PO_4)^{3-}$ orthophosphate tetrahedral [12]. The intensity of the band diminishes for the composition with highest CdI_2 content (20%).

The common feature observed from spectroscopic investigation of silver phosphate glass-nanocomposites of different categories is that the vibrational bands present in the undoped and CdI_2 doped compositions are the same. This implies that the insertion of CdI_2 cannot modify the basic phosphate network drastically. It should be mentioned that Raman spectroscopic studies of some PbI_2 or HgI_2 doped silver phosphate glasses revealed that the basic glass network remained unchanged with the insertion of these metal halides [1,2].

Fig. 5(a) shows the DSC curves for several compositions of $y = 0.40$ series. The samples show the endothermic baseline shift due to glass transition. The glass transition temperature (T_g) was obtained from these curves. In a similar manner T_g for other compositions were also estimated. Fig. 5(b) shows the compositional dependence of T_g. It is observed that the glass transition temperature increases with the increase of CdI_2 content. Similarly, glass transition temperature also increases with increase of P_2O_5 content (when CdI_2 content is fixed) for most of the compositions. The increase of glass transition temperature generally depends on the chain length of phosphate glasses, cross-link density and

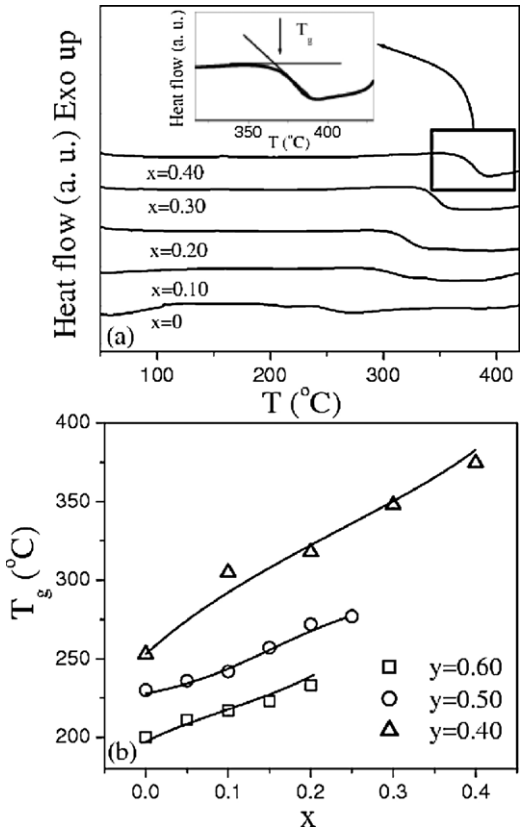

Fig. 5. (a) DSC curves for different compositions of $x\mathrm{CdI_2}$–$(1-x)(0.40\mathrm{Ag_2O}$–$0.60\mathrm{P_2O_5})$. (b) Compositional dependence of the glass transition temperature for $x\mathrm{CdI_2}$–$(1-x)(y\mathrm{Ag_2O}$–$(1-y)\mathrm{P_2O_5})$ glass nanocomposites.

nature of bonding [17]. It has been reported that the ultraphosphate glasses consist of 3D cross-linked network [4], which increases T_g. However, the dependence of T_g on dopant salts is quite complex. It has been observed for PbI_2 or HgI_2 doped silver phosphate glasses that glass transition temperature decreases with increase of respective dopants [2]. The decrease of T_g with increase of CdI_2 content was also observed in $(CdI_2)_x$–$(AgPO_3)_{(1-x)}$ glasses for $x = 0.05$ and 0.10 in contradiction to our findings [19]. However, the nature of decrement was sharp in case of PbI_2 doped glasses and linear for HgI_2 doped glasses. This complex behavior of glass transition temperature has been attributed to the cation polyanion $(PO_3)_n^n$ interaction, which governs the polyanions mobility [2]. When metal (M) iodide is doped in the phosphate network, P—O—M bond is formed. Strength of the bond depends on character of M and generally covalent nature of bond increases its strength [17]. Hg interacts weakly with oxygen and does not form covalent bond [20]. Whereas both Cd^{2+} and Pb^{2+} cation can form covalent bond with oxygen i.e. P—O—Pb and P—O—Cd bonds have covalent character [21], although the variation of glass transition temperature with respect to PbI_2 and CdI_2 mol fraction is just opposite. At present it is difficult to explain this complex behavior. However, it has been observed that Pb^{2+} cations can play dual role, one as a network former (when Pb—O bond is covalent) and other is network modifier (when Pb—O bond is mostly ionic) [22]. Thus the glass transition temperature in PbI_2 doped glasses might be dependent on the ratio of the two different types of Pb—O bond present in the network. On the other hand, P—O—Cd bond is covalent and thus the rigidity of the glass network is enhanced. Hence, the increase of glass transition temperature with the increase of CdI_2 content is quite reasonable for the CdI_2 doped glasses compared to PbI_2 doped glasses.

It has been observed that AgI particles of average size 10 nm are dispersed within the glassy matrix for AgI based glasses [4]. These particles form an aggregation or cluster when the AgI content is increased or the glass is heat treated [23]. These clusters weaken the glass network and the glass transition temperature decreases with the increase of AgI content [24] in sharp contrast to the present CdI_2 doped glasses. Although, there are several nano-sized phases present in the compositions, the presence of CdI_2 aggregation for CdI_2 rich composition should specially be mentioned. This indicates that the nanocrystalline phases do not affect the basic glass network.

The electrical properties of the present glass compositions were reported and compared with those of PbI_2 or HgI_2 doped $AgPO_3$ glass earlier [3]. The conductivity of the compositions increases with increase of CdI_2 content for poly and metaphosphate glasses, whereas the conductivity decreases for ultraphosphate compositions with increase of CdI_2 content [3]. For poly and metaphosphate system the exchange reaction between CdI_2 and AgI is complete and maximum of Ag^+ ions are located in iodine environment. On the other hand, in ultraphosphate system the exchange reaction between CdI_2 and Ag_2O is not complete and some unreacted CdI_2 is present which affects the ionic motion [3]. It should be noted that the degree of exchange between immobile cation (like Pb^{2+}, Cd^{2+}, Hg^{2+}) and Ag^+ ion depends on the type of the immobile cation [3]. Depending on the degree of exchange the conductivity may increase or decrease. For instance, the degree of exchange between Pb^{2+} and Ag^+ is higher than that between Cd^{2+} and Ag^+ or Hg^{2+} and Ag^+ [3]. That is why the conductivity of PbI_2 doped $AgPO_3$ glass is higher than that of CdI_2 or HgI_2 doped $AgPO_3$ glass.

4. Conclusions

Although CdI_2 doped silver phosphate glasses are X-ray amorphous in nature, TEM micrographs show the presence of several crystalline phases like CdI_2, AgI, $AgPO_3$ and $Ag_4P_2O_7$ dispersed in the glass matrix. The presence of CdI_2 nanoparticles in cluster form is dominant for the compositions in the limit of the glass forming domain. The size of those particles depends on the type of the phosphate network. The particle size is higher for polyphosphate compositions than that for metaphosphate or ultraphosphate compositions. The presence of different nanocrystalline phases does not affect the basic glass network. However, the insertion of CdI_2 increases the rigidity of the glass network as confirmed from DSC and infrared studies. This feature is different from what has been observed for PbI_2 or HgI_2 doped glasses.

References

[1] J. Swenson, A. Matic, C. Gejke, L. Börjesson, W.S. Howells, M.J. Capitan, Phys. Rev. B 60 (1999) 12023.
[2] J.P. Malugani, R. Mercier, M. Tachez, Solid State Ion. 21 (1986) 131.
[3] S. Kabi, A. Ghosh, Solid State Ion. 187 (2011) 39.
[4] R.K. Brow, J. Non-Cryst. Solids 263–264 (2000) 1.
[5] G. El-Damrawi, A.K. Hassan, H. Doweidar, Physica B 291 (2000) 34.
[6] M. Tatsumisago, N. Torata, T. Saito, T. Minami, J. Non-Cryst. Solids 196 (1996) 193.
[7] S. Kabi, A. Ghosh, J. Phys. Chem. C 115 (2011) 9760.
[8] JCPDS-ICDD Card No. 40-1469, 40-1468,11-0641,11-0642,7783-96-2,37-0187, 22-1192, 1993.
[9] R. Popovitz-Biro, N. Sallacan, R. Tenne, J. Mater. Chem. 13 (2003) 1631.
[10] J.K. Pike, H. Byrd, A.A. Morrone, D.R. Talham, J. Am. Chem. Soc. 115 (1993) 8497.
[11] J. Soderlund, L.B. Kiss, G.A. Niklasson, C.G. Granqvist, Phys. Rev. Lett. 80 (1998) 2386.
[12] A.M. Efimov, J. Non-Cryst. Solids 209 (1997) 209.
[13] K. Meyer, J. Non-Cryst. Solids 209 (1997) 227.
[14] R.F. Bartholomew, J. Non-Cryst. Solids 7 (1972) 221.
[15] M. Abid, M. Et-tabirou, M. Taibi, Mater. Sci. Eng. B 97 (2003) 20.
[16] R.C. Lucacel, A.O. Hulpus, V. Simon, I. Ardelean, J. Non-Cryst. Solids 355 (2009) 425.
[17] P. Singh, S.S. Das, S.A. Agnihotry, J. Non-Cryst. Solids 351 (2005) 3730.

[18] S.S. Das, B.P. Baranwal, P. Singh, V. Srivastava, Progr. Cryst. Growth Charact. 45 (2002) 89.
[19] H. Takahashi, H. Nakanii, T. Sakuma, Solid State Ion. 176 (2005) 1067.
[20] A.K. Prokof'ev, Russ. Chem. Rev. 50 (1981) 32.
[21] M.E. Hezzat, M. Et-tabirou, L. Montagne, E. Bekaert, G. Palavit, A. Mazzah, P. Dhamelincourt, Mater. Lett. 58 (2003) 60.
[22] E. Husson, J.M. Bény, C. Proust, R. Benoit, R. Erre, Y. Vaills, K. Belkhader, J. Non-Cryst. Solids 238 (1998) 66.
[23] N. Itakura, M. Tatsumisago, T. Minami, J. Am. Ceram. Soc. 80 (1997) 3209.
[24] B.V.R. Chowdari, R. Gopalakrishnan, J. Non-Cryst. Solids 105 (1988) 269.